Sulfides and Oxides in Fe-Mn Alloys: Part III. Formation of Oxysulfides during Freezing of Steel

G. J. W. KOR AND E. T. TURKDOGAN

The previous study of the phase relations (Part I) is now extended to the solid-liquid regions of Fe-Mn-S and Fe-Mn-S-O systems. The differential thermal analysis measurements made with 1 to 5 pct Mn-Fe alloys containing sulfur and oxygen substantiated the positions of the univariant curves in pct Mn vs T plots derived from other available data and theoretical considerations. It is found that if sufficient oxygen and sulfur are present in the Fe-Mn alloys, there may be a liquid oxysulfide phase present at temperatures above 900°C, depending on the manganese content. The higher the manganese content in solution, the higher is the temperature below which no liquid phase is present, *e.g.* for 10 ppm, 900°C and for 10 pct Mn, ~1200°C. The formation of oxides, sulfides, and liquid oxysulfides in the interdendritic regions during solidification, as predicted from the phase relations in the Fe-Mn-S-O system, was verified by microscopic examination using scanning electron microscopy and metallographic techniques.

IN Part I of this series of papers, Turkdogan and Kor[1] discussed phase relations in the Fe-Mn-S-O system derived from the available data by applying the Morey-Williamson theorem on univariant curves intersecting at an invariant point. The previous study is now extended to the solid-liquid regions of Fe-Mn-S and Fe-Mn-S-O systems. Some of the calculated univariant equilibria were tested by differential thermal analysis (DTA) of Fe-Mn alloys containing sulfur and oxygen. Using these phase equilibria some consideration is given to the formation of sulfide and oxysulfide inclusions during solidification of steel.

PHASE EQUILIBRIA

For the present purpose it is convenient to show the phase relations in the Fe-Mn-S and Fe-Mn-S-O systems by plotting the equilibrium manganese activity (represented by concentration in the solid metal) against temperature for univariant equilibria involving the solid metal (γ- or δ-phase). Such a plot is shown in Fig. 1 for the Fe-Mn-S system. The ternary eutectic invariant I is at 980°C where γ-iron, "FeS", and liquid metal (l_2) are in equilibrium. The outer curve k on the right is the solidus curve for the binary Fe-Mn system.

The univariant a for γ-iron, "MnS", and liquid (l_2) equilibrium is calculated from the collated data discussed previously.[1] The derivation of univariant b for δ-iron, "MnS", and l_2 is based on two major assumptions:

i) The liquidus of the alloy is a linear function of composition for alloys containing Mn < 12 pct and S < 3 pct, thus

$$T(\mathrm{K}) = 1810 - 5.0[\%\mathrm{Mn}]_l - 14.3[\%\mathrm{S}]_l \qquad [1]$$

where the coefficients 5.0 and 14.3 are for the δ-iron region of the Fe-Mn and Fe-S binary systems respectively.

ii) The manganese distribution ratio between δ-iron and the liquid for the Fe-Mn system[2] applies also to the Fe-Mn-S system, thus

$$\frac{[\%\mathrm{Mn}]_s}{[\%\mathrm{Mn}]_l} = 0.74 \qquad [2]$$

The equilibrium constant for the Mn-S reaction in the liquid phase is represented by

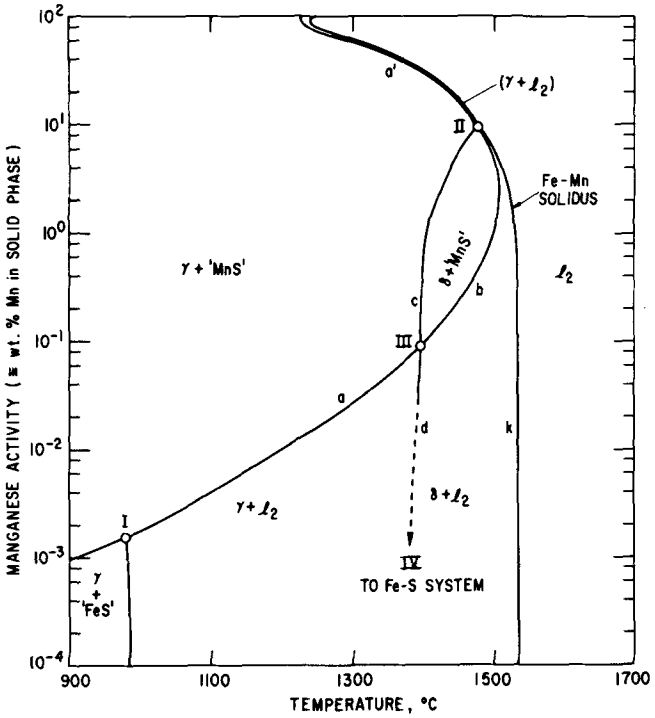

Fig. 1—Univariant equilibria involving solid metal in Fe-Mn-S system bounded with binary Fe-S and Mn-S terminal-phase fields. (*a*) γ, "MnS" l_2; (*b*) δ, "MnS", l_2; (*c*) δ, γ, "MnS"; (*d*) δ, γ, l_2

G. J. W. KOR and E. T. TURKDOGAN are Senior Scientist and Manager, respectively, Chemical Metallurgy Division, U. S. Steel Corp. Fundamental Research Laboratory, Research Center, Monroeville, Pa.

Manuscript submitted October 11, 1971.

$$MnS(s) = \underline{Mn}(1 \text{ wt pct}) + \underline{S}(1 \text{ wt pct}) \quad [3]$$

At the manganese concentrations considered the activity $a_{MnS} \simeq 1$, hence

$$k' = [\%Mn]_l [\%S]_l \quad [4]$$

From the available equilibrium data,[3] the temperature dependence of k' is given by

$$\log k' = -\frac{8236}{T} + 5.03 \quad [5]$$

The univariant b in Fig. 1 is derived by simultaneous solution of Eqs. [1], [2], [4], and [5]. This univariant has a temperature maximum and terminates at the Mn-MnS eutectic at 1230°C after passing through the δ-γ transformation. The early workers[4-6] did in fact show qualitatively several maxima and minima on the primary liquidus surfaces of the δ and "MnS" phases in this ternary system. Using the equations given above, the temperature maximum ($dT/d[\%Mn]_s = 0$) is estimated to be at 1510°C and 2 pct Mn in the δ phase. The alloy composition thus estimated for this temperature maximum can be checked by applying the Morey-Williamson theorem.[7]

According to the Morey-Williamson theorem (examples of its application are given elsewhere[1,8]), a temperature maximum or a minimum on the univariant curve indicates that the compositions of the three condensed phases involved are colinear in a ternary system. The iron-rich side of the Fe-Mn-S phase diagram is shown in Fig. 2 where the liquid miscibility gap univariant and the eutectic univariant are projected on the composition plane. At the temperature maximum, the compositions of δ-iron, liquid metal, and MnS are colinear as indicated by the dotted curve. Representing the composition of the liquid at M by $[\%Mn]_l$ and $[\%S]_l$ and that of the solid by $[\%Mn]_s$ (the trace amount of sulfur in δ phase is neglected), the following expression is derived from geometric considerations and the composition of MnS in wt pct,

$$\frac{36.8}{[\%S]_l} = \frac{63.2 - [\%Mn]_s}{[\%Mn]_l - [\%Mn]_s} \quad [6]$$

Substituting Eqs. [2] and [4], Eq. [6] simplifies approximately to

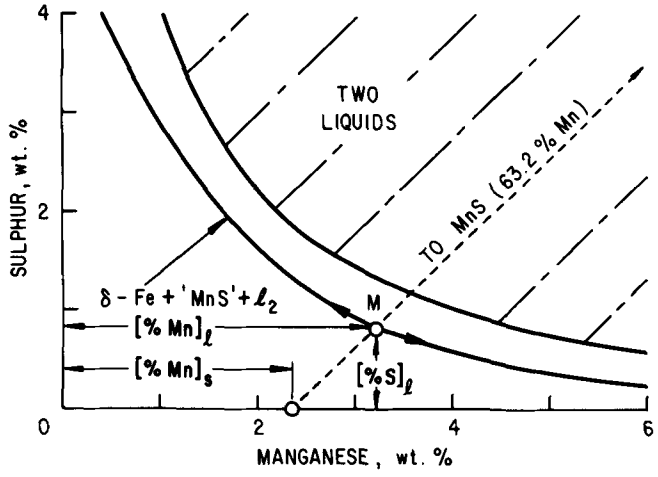

Fig. 2—Projected univariants for the miscibility gap and the eutectic in part of the Fe-Mn-S system; a temperature maximum on the eutectic univariant is indicated.

$$[\%Mn]_s \simeq 1.9\sqrt{k'} \quad [7]$$

Now, inserting the value of k' for the temperature maximum 1510°C gives $[\%Mn]_s = 3$ which is only 50 pct greater than the value estimated using Eq. [1]. By combining Eq. [7] with those given earlier the temperature maximum is estimated to be at 1508°C, $[\%Mn]_s = 3$, $[\%Mn]_l = 4$ and $[\%S]_l = 0.8$.

Because of the low sulfur content of the solid metal in equilibrium with "MnS", the univariant c in the %Mn vs T plot would be similar to that of the γ-δ phase boundary of the Fe-Mn system. By the same token, the invariant II involving γ phase, δ phase, "MnS", and liquid metal is placed close to the peritectic invariant of the Fe-Mn system at 1474°C where the equilibrium sulfur content of the solid metal with 9 pct Mn is about 8 ppm.

In evaluating the invariant point III, again involving γ phase, δ phase, "MnS", and liquid metal, use is made of the corresponding peritectic invariant for the Fe-S system at 1365°C where the sulfur contents of the phases are:[9] 0.05 pct S in γ-iron, 0.18 pct S in δ-iron and 12 pct S in the liquid phase. Also, the location of the invariant III in the %Mn vs T plot must satisfy the MnS solubility in γ-iron such that at this invariant, %S < 0.05 and temperature > 1365°C. Using the MnS-solubility data of Turkdogan *et al.*,[10] the invariant III is placed at 1395°C and 0.1 pct Mn for which the equilibrium sulfur in γ-iron is about 0.038 pct.

As indicated by an arrow in Fig. 1, the univariant d terminates at the invariant point IV of the Fe-S binary system.

The invariant involving δ-Mn in the manganese-rich alloys near 1225°C is not included in Fig. 1.

The univariant equilibria involving $\gamma(\delta)$-iron and

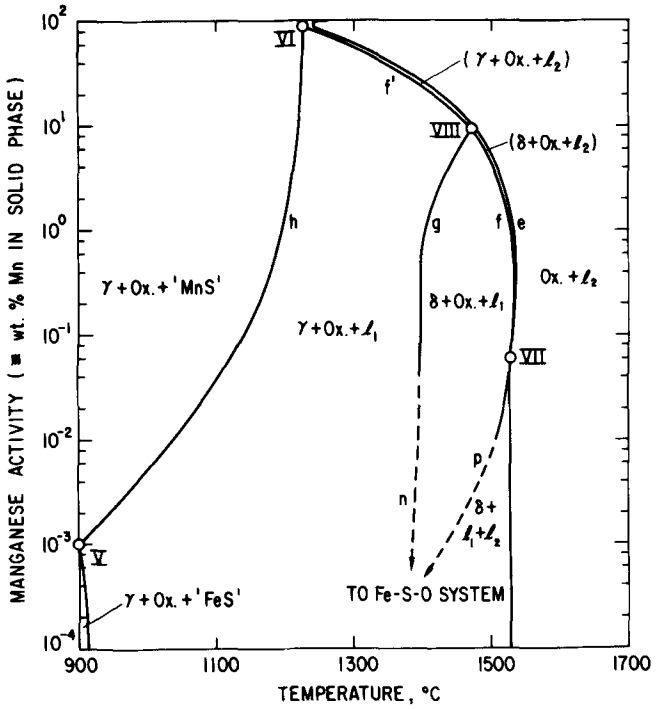

Fig. 3—Univariant equilibria involving solid metal and Mn(Fe)O in Fe-Mn-S-O system bounded with ternary Fe-Mn-O and Fe-S-O terminal-phase fields. (*e*) δ, Ox., l_2; (*p*) δ, l_1, l_2; (*f*) δ, Ox., l_1, l_2; (*n*) δ, Ox., l_1, l_2; (*g*) δ, γ, Ox., l_1; (*h*) γ, Ox., "MnS", l_1.

"MnO" in the Fe-Mn-S-O system with ternary Fe-Mn-O and Fe-S-O terminal phase fields are given in Fig. 3. The univariant curves intersecting at the invariant points V and VI for the quaternary system are those estimated previously by the authors.[1] The univariant f terminated at VII which is the liquid miscibility gap invariant for the Fe-Mn-O system at 1527°C assumed to be nearly the same as that for the binary Fe-O miscibility gap invariant. The equilibrium phases at the invariant VII are: δ-iron, Mn(Fe)O, liquid oxide (l_1), and liquid metal (l_2).

The equilibrium phases along univariant e for the Fe-Mn-O system are: δ-iron, "MnO", and l_2. Because of the relatively low MnO solubility product, at manganese contents above 1 pct the equilibrium oxygen in solution is too small to affect noticeably the liquidus or solidus temperatures of the Fe-Mn alloys. For example, at 1527°C, for melt in equilibrium with essentially pure MnO, the product [%Mn] × [%O] = 0.025; for melt containing 1 pct Mn, the equilibrium oxygen in solution is 0.025 pct which lowers the melting point of the alloy by about 1° to 2°C. In other words, the univariant e above about 1 pct Mn is essentially the same as the solidus curve of the Fe-Mn binary system. However, below 1 pct Mn a small correction is made to the solidus temperature of the Fe-Mn system to account for the increasing effect of oxygen on the melting temperature. The univariant g for the $\delta \rightarrow \gamma$ transformation is again assumed to be similar to that of the Fe-Mn binary system. As indicated by arrows, dotted curves terminate at the Fe-S-O ternary system.

A similar diagram is drawn in Fig. 4 for univariant equilibria involving γ(δ)-iron and "MnS" in the Fe-Mn-S-O system with ternary Fe-Mn-S and Fe-S-O and binary Fe-Mn terminal phase fields. For small amounts of sulfur and oxygen, the solidus temperature of the quaternary system will not differ much from that of the Fe-Mn system which is shown by the univariant k. Because of the low oxygen solubility in Mn(Fe)S, the univariants a and b for the γ(δ)-iron, "MnS", and liquid (l_1 or l_2) equilibria are reproduced from Fig. 1 for the Fe-Mn-S ternary system. For the sake of simplicity, the $\delta \rightarrow \gamma$ transformation is omitted in this equilibrium diagram. In the presence of oxygen, the three-phase equilibrium (γ, "MnS", l_2) is spread within a narrow field between the curves b and j as shown in Fig. 4.

The univariant j is for the quaternary system involving phases γ(δ)-iron, "MnS", liquid oxysulfide (l_1) and liquid metal (l_2). This liquid miscibility gap univariant starts from the invariant VI and terminates on univariant a-b again for the quaternary system. It should be noted that although there is a liquid miscibility gap univariant in equilibrium with MnS in the Fe-Mn-S system, it does not form an invariant point. Because of the low oxygen content of the metal for manganese > 1 pct, the melting point for j should be only slightly below that for the univariant b.

The terminal two-phase regions γ + "FeS", γ + l_1, and γ + l_2 at low manganese contents are for the ternary Fe-S-O system. The liquid miscibility gap univariant m for this system starts at 1345°C (which is taken to be the terminal point for j) and approaches the Fe-O invariant (1527°C) asymptotically. At higher manganese contents the two-phase region γ + l_2 is for the ternary Fe-Mn-S system.

DIFFERENTIAL THERMAL ANALYSIS

Parts of the univariant curves f, g, and h in Fig. 3 for (Mn, Fe)O-saturated Fe-Mn-S-O system were checked by carrying out differential thermal analysis on Fe-Mn alloys containing sulfur and oxygen.

Three iron alloys were investigated; they were prepared in a small vacuum-melting furnace using Plastiron as the base material. The melts were chill-cast in copper molds of 10 cm length and 2.5 cm diam; the compositions of the alloys investigated are given in Table I.

The differential thermal analysis was carried out in a standard commercial apparatus. For each experi-

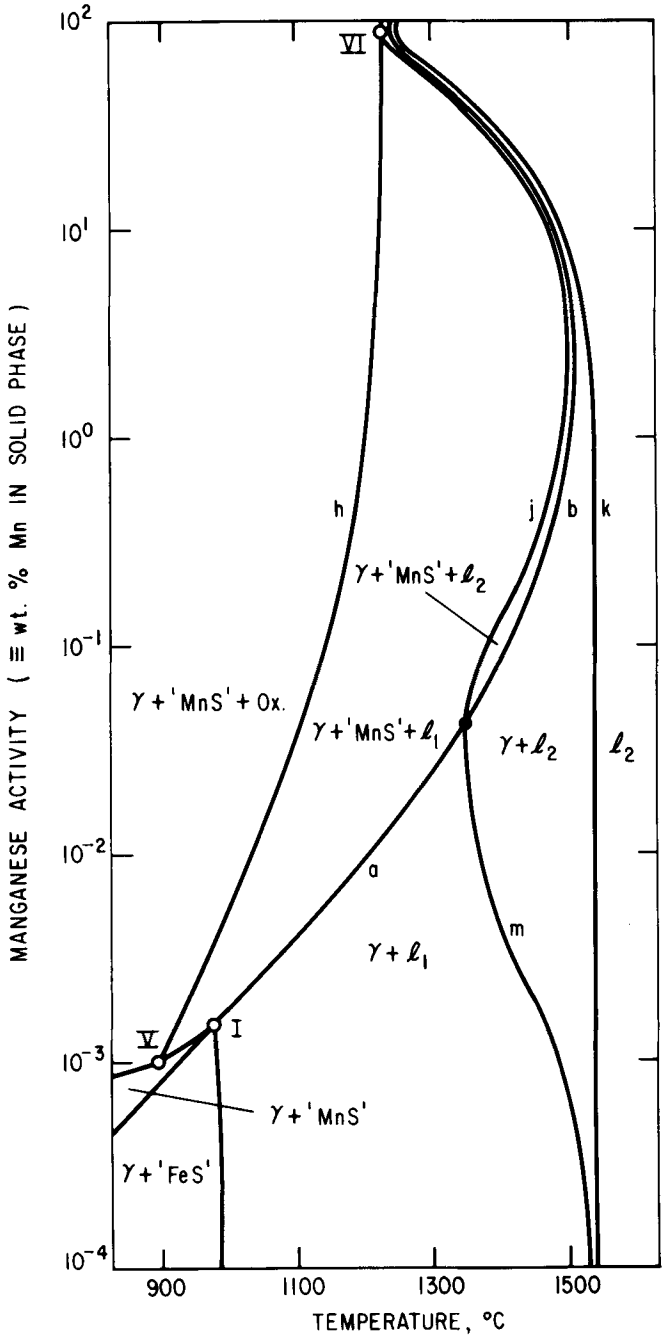

Fig. 4—Univariant equilibria involving solid metal and "MnS" in Fe-Mn-S-O system with ternary Fe-Mn-S and Fe-S-O and binary Fe-Mn terminal-phase fields. (j) γ, "MnS", l_1, l_2; (m) γ, l_1, l_2; (k) γ, l_2

Table I. Composition of Iron Alloys (Wt. Pct) Used for Differential Thermal Analysis

Alloy No	Pct Mn	Pct S	Pct O
1	4.8	0.14	0.015
2	3.3	0.53	0.008
3	1.1	0.17	0.030

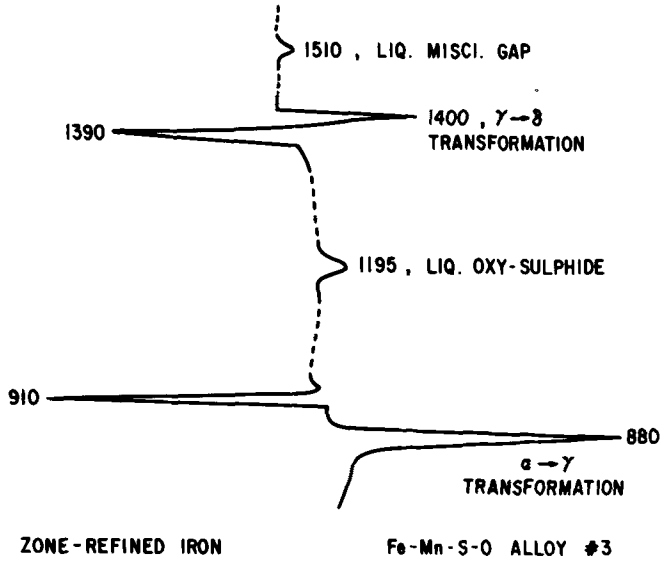

Fig. 5—DTA diagram showing phase changes in reference sample (peaks on right); numbers indicate temperature in degrees centigrade.

ment two specimens were used: an iron alloy and a reference specimen of high-purity zone-refined iron, both having a height of 7 mm and a diameter of 3 mm, and weighing about 0.4 g. The Pt-Pt/10 pct Rh thermocouple, with a thin alumina protection sheath, was inserted snugly into a hole in the specimen.

After the alloy and the reference specimen were mounted in place, the reaction tube of the furnace was flushed with argon, purified by passing over heated titanium chips. After flushing for several hours, the furnace was heated at a constant rate of 10°C per min, while the gas was kept flowing to prevent oxidation of the specimens. The temperatures were always determined from heating curves using the known transformation temperatures of pure iron, obtained from the reference sample, as "calibration points". Fig. 5 shows a typical DTA curve, obtained for alloy No. 3, showing the transformation peaks for the alloy (right) and the zone-refined iron (left) as well as the two small peaks indicating the formation of liquid oxysulfide, l_1(1195°C), and liquid metal, l_2(1510°C). On repeated experiments the arrest temperatures were reproducible within about 5°C.

The area under a peak in a DTA curve is proportional to the enthalpy change accompanying the phase transformation or the reaction which gives rise to the peak.[11,12] The areas under the peaks recorded for the alloy, peaks on the right in Fig. 5, were measured with a planimeter. The peak area at 1195°C is 13 pct of that at 880°C; it is therefore deduced that the enthalpy change accompanying the formation of the liquid oxysulfide (l_1) from solid "MnO" and "MnS" is 13 pct of

Table II. Transformation Temperatures and Temperatures (°C) at Which l_1 and l_2 Were Formed, Obtained from DTA Heating Curves

Alloy No	Pct Mn in Solid Solution	$T(\alpha\gamma)$	$T(l_1)$	$T(\gamma\delta)$	$T(l_2)$	Remarks
1	4.50	775	1210	1445	1503	Avg. of 3 runs.
2	2.40	820	1210	1420	1500	1 run.
3	0.64	880	1195	1400	1510	Avg. of 3 runs.

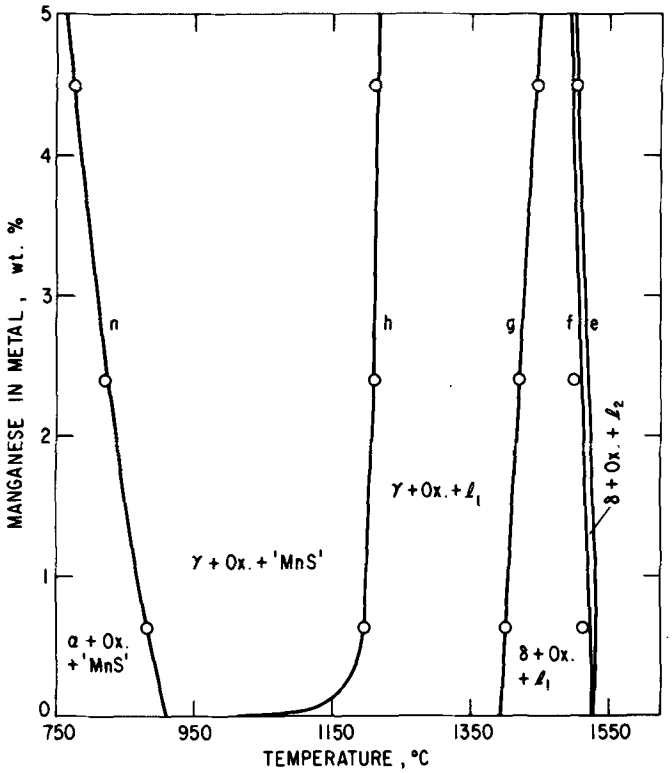

Fig. 6—Results of DTA measurements are compared with calculated univariant curves for oxide-saturated Fe-Mn-S-O system, partially reproduced from Fig. 3.

the enthalpy change for $\alpha \rightarrow \gamma$ transformation. Assuming an ideal solution, the enthalpy of formation of l_1 from solid oxides and sulfides of iron and manganese for the alloy considered is estimated to be 8.5 kcal per mole. From the sulfur and oxygen contents of the alloy No. 3, the amount of l_1 formed is estimated to be 0.4 wt pct. Based on the specimen weight of 0.4 g, the enthalpy change for the $\alpha \rightarrow \gamma$ transformation is 1.5 cal and that for l_1 about 0.17 cal, which is 11 pct of that for the $\alpha \rightarrow \gamma$ transformation, in good agreement with that derived from the relative areas of the corresponding DTA peaks.

The arrest temperatures for the three alloys investigated are given in Table II. Because of the formation of oxides and sulfides, the manganese in solid iron is less than the total amount of manganese in the alloy; estimated pct manganese in solution is given in Table II.

Parts of univariant curves h, g, f, and e from Fig. 3 are reproduced in Fig. 6 together with the α-γ phase boundary, n, for the Fe-Mn system from the work of Troiano and McGuire;[13] it should be recalled from the previous discussion that univariants e and h are for solidus and δ-γ transformation in the binary

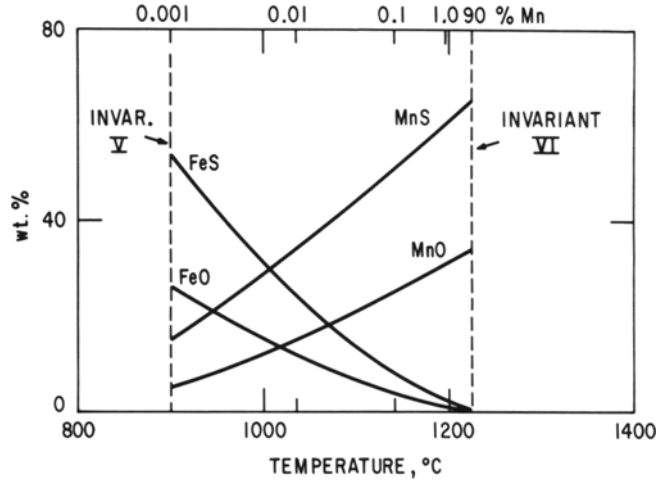

Fig. 7—Calculated composition of liquid oxysulfide in equilibrium with "MnO"-saturated γ-iron containing Mn, O, and S.

Fe-Mn system[2] approximated to the Fe-Mn-S-O system considered. The results from the DTA measurements do indeed substantiate the approximations made in the estimation of univariants h and f and application of the univariants e, g, and n of the binary Fe-Mn system to the quaternary Fe-Mn-S-O system.

Hilty and Crafts[14] investigated parts of the Fe-Mn-S-O system by microscopic examination of quenched samples. They place the miscibility gap invariant f for oxide-saturated alloy containing 1 pct Mn at 1475°C, which is about 35° to 45°C lower than that found in the present work. Because of the nature of the experimental technique, employed by Hilty and Crafts, their melt was apparently not in equilibrium with the container made of Fe-1 pct Mn alloy. For this univariant the estimated manganese content in solid iron is about 9 pct at 1475°C.

As pointed out earlier, the univariant h was derived in Part I on the assumption of an ideal solution, and by the same token the composition of the liquid oxysulfide was shown to be calculable. The results of the calculations are given in Fig. 7 where the composition of the liquid oxysulfide for univariant h, represented in terms of FeO, FeS, MnO, and MnS, is shown as a function of temperature (bottom scale) and the corresponding equilibrium pct manganese in the γ phase (top scale).

FORMATION OF SULFIDE AND OXYSULFIDE INCLUSIONS

Unlike oxygen, the sulfur content of steel is controlled primarily during the steelmaking operation; normally, no desulfurization is carried out in the ladle prior to casting. Assuming that there are no entrapped slag particles in the metal stream, all the sulfur is in solution in steel at the time of casting. The sulfide inclusions are formed in the interdendritic liquid during solidification in a manner similar to that discussed previously[15] for the formation of interdendritic oxide and silicate inclusions. However, there are certain characteristic features of the formation of sulfide and oxysulfide inclusions which deserve closer examination. For better understanding of the formation of oxysulfides, studies were made of Fe-S-O, Fe-Mn-S-C, and Fe-Mn-S-O alloys.

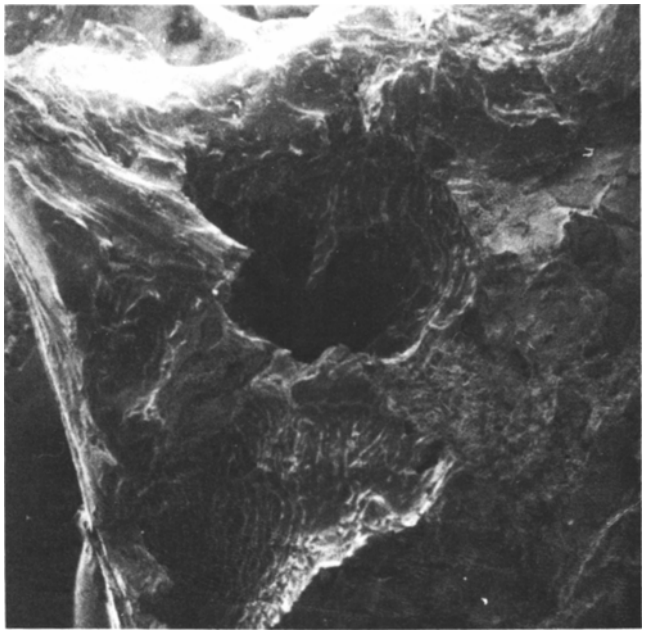

(a)

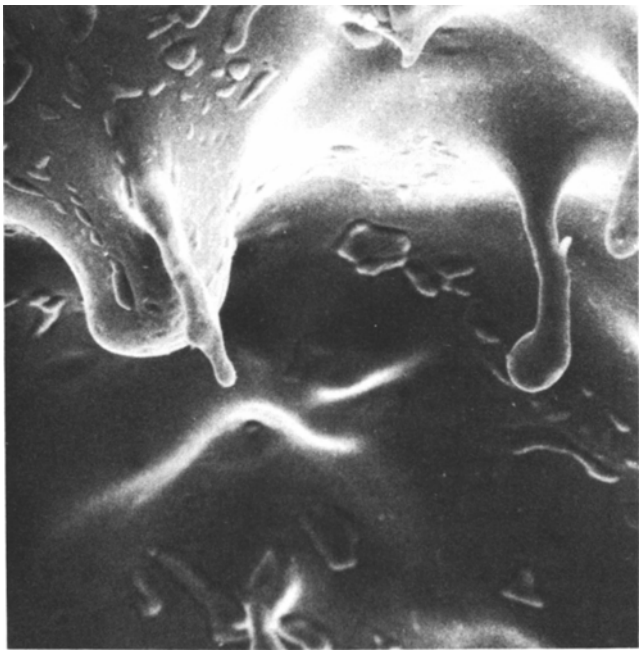

(b)

Fig. 8—Blowhole on the fracture surface (*a*) of Fe-0.14 pct S-0.04 pct O alloy; inside wall of this blowhole (*b*) as viewed in the scanning electron microscope showing patches believed to be liquid oxysulfide formed during freezing.

Fe-S-O System

Before discussing the results of the present investigation, it should be pointed out that Yarwood *et al.*[16] investigated the formation of liquid oxysulfides in the interdendritic liquid during freezing of Fe-S-O melts. The present findings reported briefly in this paper are in general accord with those of Yarwood *et al.*

Liquid (plastiron) iron containing 0.04 pct O and 0.14 pct S was cast in a 7 by 7 by 20 cm ingot mold, and representative samples were examined by the metallographic microscope and the fracture surfaces were viewed in the scanning electron microscope.

According to the work of Hilty and Crafts,[17] the liquid miscibility gap univariant in equilibrium with γ iron closes at about 1345°C where the liquid phase contains about 2 pct O and 17 pct S. That is, in alloys with the usual oxygen and sulfur levels with %O/%S > 0.12, two liquids may form over a certain range of temperature and composition. In the alloy investigated in the present work, the ratio %O %S is about 0.29, indicating that the interdendritic liquid may separate into two liquid phases during freezing of the alloy. The Fe-S-O alloy investigated contained about 0.02 pct C, and as a result many blowholes were present in the cast ingot. The top picture in Fig. 8 shows at low magnification a large blowhole exposed on the fracture surface. Closer examination of the inside of the hole at a higher magnification (bottom picture) reveals the presence of the liquid oxysulfide droplets that spread on the inner wall of the blowhole during freezing.

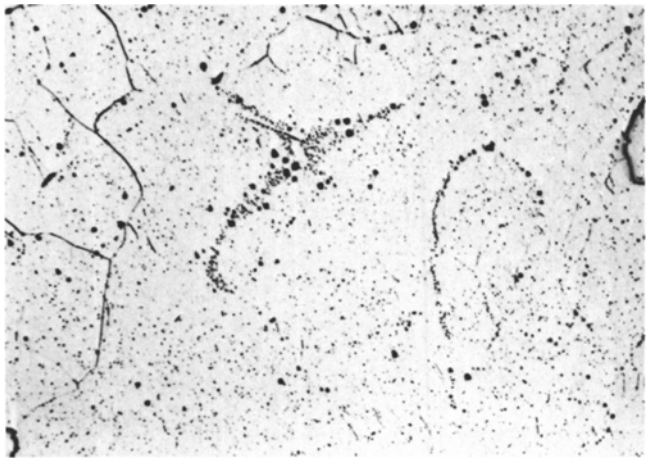

Fig. 9—Oxide and sulfide precipitates in the interdendritic regions of Fe-0.14 pct S-0.04 pct O alloy.

The light micrograph in Fig. 9 is a typical view of the cross section showing essentially uniform distribution of oxide and sulfide particles with clustering at some original grain boundaries. The secondary or tertiary interdendritic regions at about 10 to 30 μm intervals are faintly outlined by the oxide and sulfide precipitates.

The micrographs in Fig. 10 are fracture surfaces at different magnifications as viewed by scanning electron microscopy. The characteristic cup and cone fractures are obtained, revealing clearly that the spheroidal particles, mostly within the range 1 to 3 μm, are distributed throughout the metal. Fig. 10(*c*) shows clearly the typical shrinkage cavity on a 6 μm diam oxysulfide particle. The white spot seen on this spherical particls is caused by the electron beam used in the fluorescent X-ray analysis of the inclusions.

To facilitate better metallographic examination of the oxysulfide inclusions, a sample of Fe-S-O alloy, enclosed in an evacuated silica capsule, was heat treated at 1200°C for 1 hr, then quenched in water. The light micrograph in Fig. 11 shows clearly the eutectic freezing of the liquid oxysulfide.

These observations substantiate the view that the sulfide, oxide, and other inclusions form readily in the enriched interdendritic liquid with little or no supersaturation for nucleation. The inclusions of the order of 1 to 3 μm or smaller diameter, distributed uniformly in the casting at 5 to 10 μm intervals, appear to have been trapped within the dendrite arms and not pushed into the interdendritic liquid during the progress of freezing; in these ingots the interdendritic spacing is within the range 50 to 80 μm. Upon annealing, however, there is appreciable growth of the liquid oxysulfide particles.

Fe-Mn-S-C System

The microsegregation and the formation of sulfide inclusions during freezing of an alloy containing 1.5 pct Mn, 0.25 pct C and 0.05 or 0.1 pct S were previously investigated by Turkdogan and Grange.[18] The basic features of the phase relations in Fig. 1 for MnS-

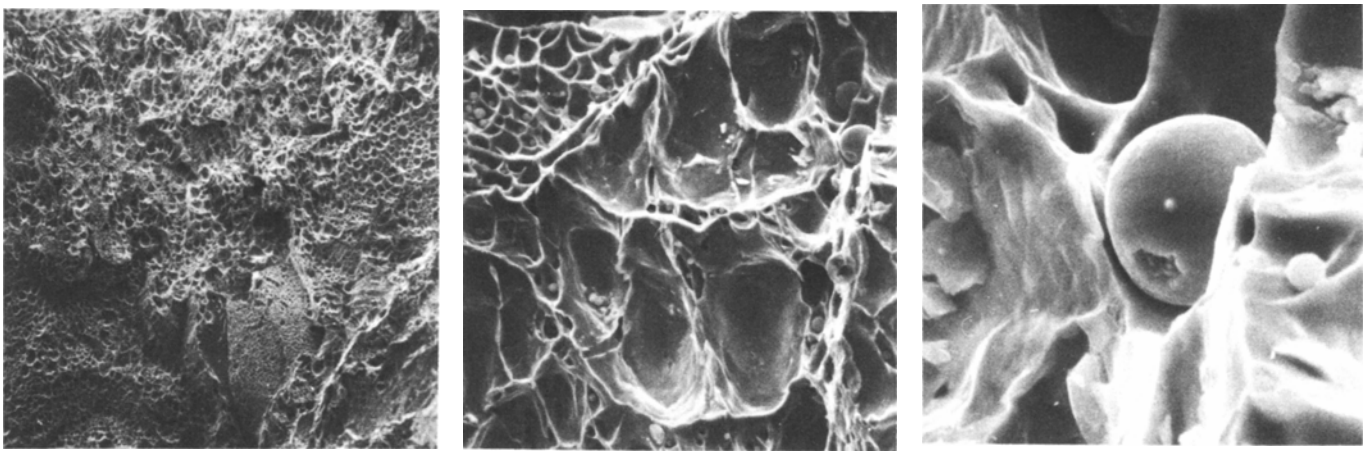

Fig. 10—Fracture surfaces of Fe-0.14 pct S-0.04 pct O alloy as viewed in the scanning electron microscope showing spheroidal oxide and sulfide inclusions at different magnifications.

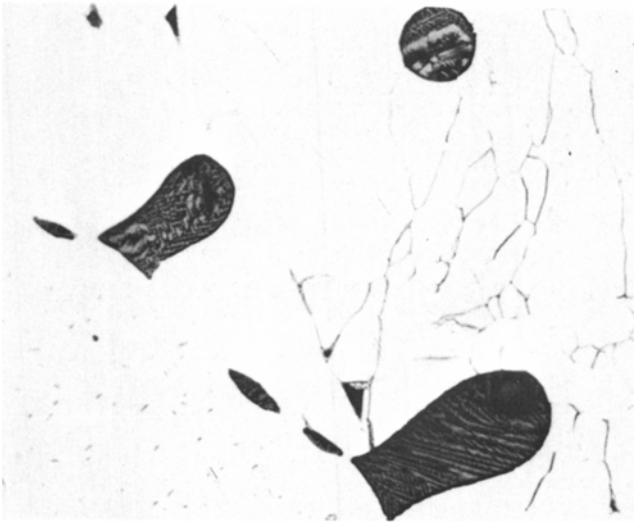

Fig. 11—Micrograph showing wustite-pyrrhotite eutectic freezing of liquid oxysulfide in Fe-0.14 pct S-0.04 pct O alloy, annealed for 1 hr at 1200°C and water quenched.

saturated Fe-Mn-S would apply even when there is some carbon in the system. In 1.5 pct Mn alloy the solid (δ) iron first formed contains about 1 pct Mn. As the solidification progresses, the manganese and sulfur contents of the interdendritic liquid increase. When the product [%Mn][%S] in the enriched liquid exceeds that of the "MnS" solubility product k', Eqs. [2] and [3], manganese sulfide inclusions are expected to form in the interdendritic liquid. For the alloy under consideration, the sulfide formation begins at 90 to 95 pct solidification as estimated by applying the Scheil equation[19] for microsegregation discussed previously.[18] At this stage of freezing the solid contains about 2 pct Mn which is below the temperature maximum on univariant b in Fig. 1. As the freezing progresses with precipitation of "MnS", the sulfur content of the enriched liquid will increase, but the manganese content of the metal will decrease along the univariant b. Finally, the last traces of the liquid rich in sulfur (~33 pct) will freeze at the eutectic invariant I (980°C). However, in relatively fast-cooled castings with low initial sulfur contents, nonequilibrium freezing may be complete before reaching the eutectic temperature. An important deduction made from this analysis is that although there is positive manganese segregation in the interdendritic region, a sharp drop in the manganese concentration in the immediate vicinity of the manganese sulfide inclusion is anticipated in alloys containing less than about 2 pct Mn.

As demonstrated previously,[18] the manganese segregation is readily observed from the microstructures of as-cast alloys containing carbon and manganese. The austenite transformation to ferrite begins in regions low in manganese, *e.g.* dendrite cores, and ultimately pearlite forms in the interdendritic manganese-rich regions. This is evident from the micrograph in Fig. 12(*a*) for fast cooling in an ingot mold. At a higher magnification, Fig. 12(*b*), we see that the manganese sulfide inclusions are embedded in a narrow ferrite band, indicating that the manganese concentration in the immediate vicinity is low relative to the neighboring interdendritic zone. Fig. 13 is for a slowly cooled casting (melt was allowed to freeze

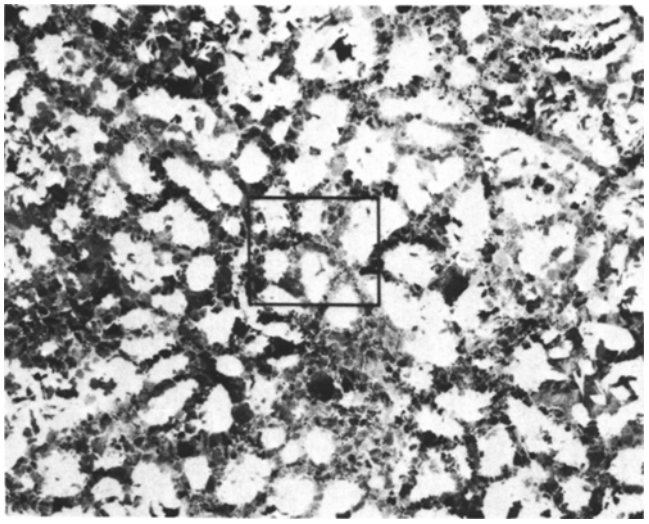

(*a*)

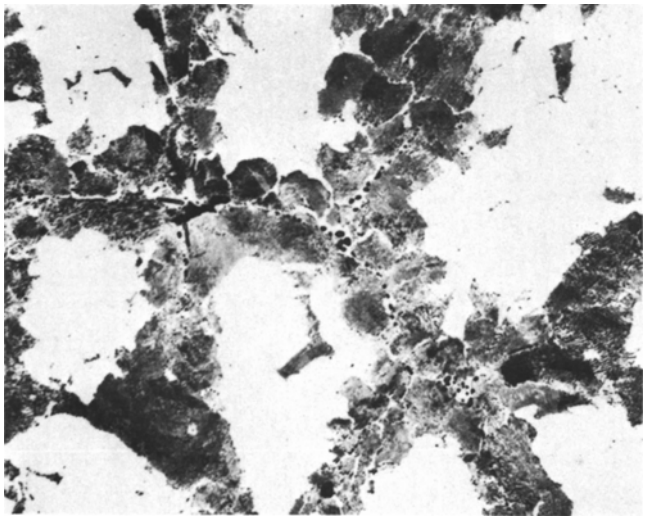

(*b*)

Fig. 12—Distribution of sulfide inclusions in fast-cooled ingot. 0.25 pct C, 1.5 pct Mn, 0.05 pct S. (*a*) Magnification 100 times. (*b*) Magnification 500 times.

in the melting crucible), again showing the sulfide inclusions in a ferrite band in the interdendritic regions; the ferrite band in the slowly cooled ingot is much wider than that in the rapidly cooled ingot. The microsegregation of manganese accompanying freezing (manganese enrichment) and that accompanying the precipitation of MnS from the melt (manganese depletion) deduced from Fig. 1 are supported by the microstructures in Figs. 12 and 13.

On the basis of the foregoing argument, it follows from the shape of the univariant b in Fig. 1 that in alloys containing more than about 2 pct Mn, the manganese sulfide inclusions will be surrounded by manganese-rich metal. Because of the etching difficulties, however, this prediction could not be verified by metallographic techniques.

Fe-Mn-S-O System

The alloy investigated contained 1.1 pct Mn, 0.17 pct S and 0.03 pct O, No. 3 in Table I. According to Eq. [6], this alloy begins to freeze at about 1529°C where

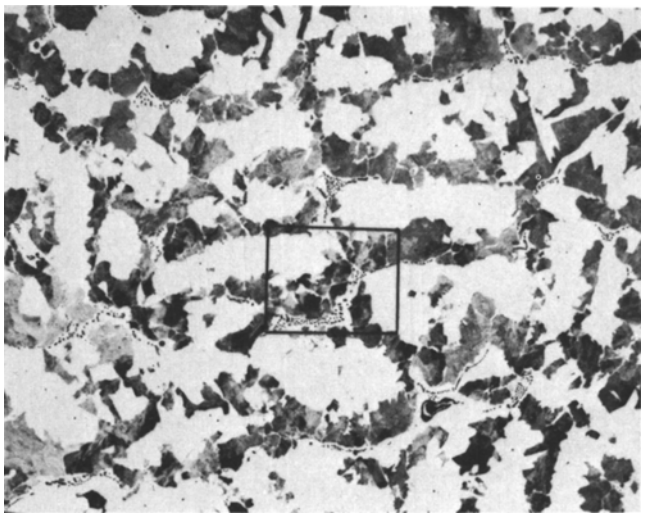

(a)

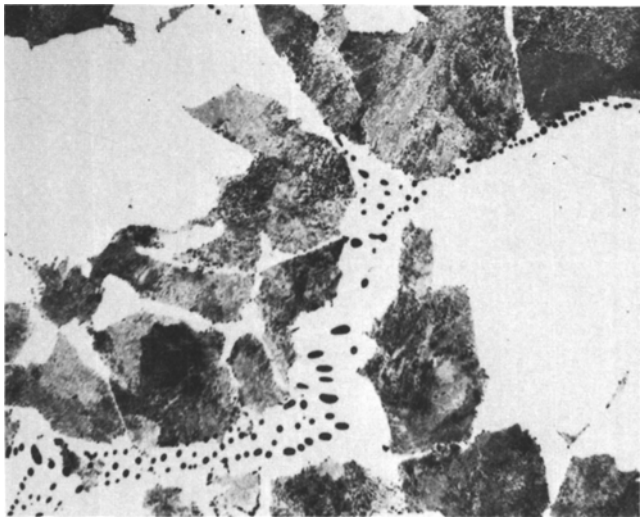

(b)

Fig. 13—Distribution of sulfide inclusions in slow-cooled ingot. 0.25 pct C, 1.5 pct Mn, 0.05 pct S. (*a*) Magnification 96 times. (*b*) Magnification 480 times.

the melt is saturated with "MnO". As the solidification progresses, more oxide (MnO with 5 to 10 pct FeO) precipitates, the concentrations of manganese and sulfur in the interdendritic liquid increase, and the corresponding manganese content of the δ phase increases within the three-phase field (δ + Ox. + l_2) bounded by univariants *e* and *f* in Fig. 3. When the composition reaches the univariant *f*, liquid oxysulfide (l_1) begins fo form. For the alloy investigated this point is reached at about 80 pct solidification when the enriched liquid contains about 1.4 pct Mn and 0.56 pct S in solution for which the estimated liquidus temperature is about 1522°C.* At this stage, most of the initial oxygen in the liquid steel is expected to be in the oxide form. As solidification progresses further, the amount of liquid oxysulfide (l_1) increases, the amount of metallic liquid (l_2) decreases, accompanied by an increase in the manganese content along univariant *f*, Fig. 3, and a corresponding decrease in the sulfur content of the metal.

*In calculating the impurity enrichment in the interdendritic liquid using the Scheil equation[19] it is assumed that there is complete mixing in the liquid, no diffusion of manganese, but complete diffusion of oxygen and sulfur in the dendrites.

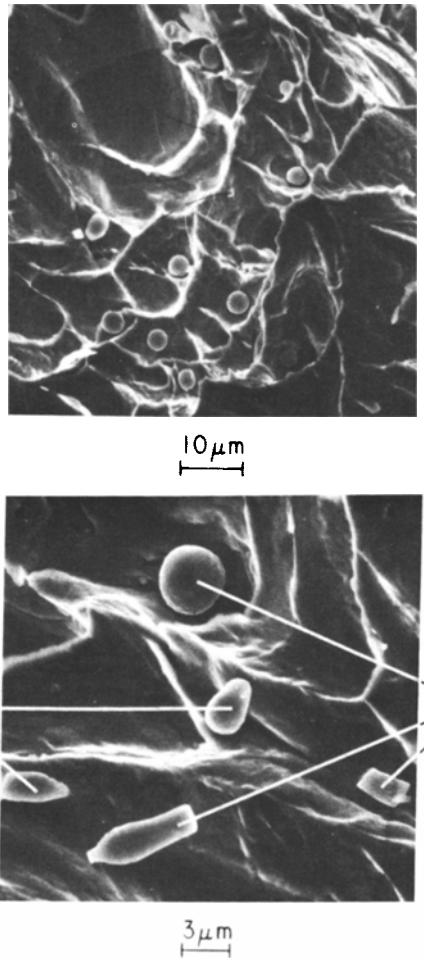

Fig. 14—Fracture surface of Fe-1.1 pct Mn-0.14 pct S-0.04 pct O alloy as viewed in the scanning electron microscope showing oxide and sulfide inclusions.

If the rate of cooling is sufficiently slow and equilibrium is maintained between the enriched liquid and MnO-saturated oxysulfide, the last metallic liquid will freeze at about 1225°C at the invariant point VI, Fig. 3, where the extension of univariant *f* (*f'*) intersects *h*. However, as discussed earlier, the oxides and sulfides forming from the enriched liquid are trapped by the growing dendrites and equilibrium is not likely to be maintained between the precipitating oxides, sulfides, and the residual liquid metal. Therefore, in the casting, nonequilibrium freezing of the last liquid metal will occur at some point on the univariant *f* below perhaps invariant VIII. Upon further cooling there is first the δ → γ transformation, and the oxysulfide saturated with MnO remains liquid until a temperature of about 1210°C is reached, *i.e.* univariant *h*, Fig. 3, where the equilibrium phases are: γ-iron, "MnO", "MnS" and l_1. Below this temperature, eutectic freezing of the liquid (l_1) gives "MnS" and more "MnO". Again, if equilibrium were to be maintained at slow cooling rates, the precipitation of MnS would continue until the eutectic invariant *V*, Fig. 3, is reached at 900°C, and the equilibrium manganese content of γ-iron in the vicinity of the oxysulfide would decrease along the univariant *h*. However, nonequilibrium eutectic freezing is likely to occur somewhere on univariant *h*, perhaps with little

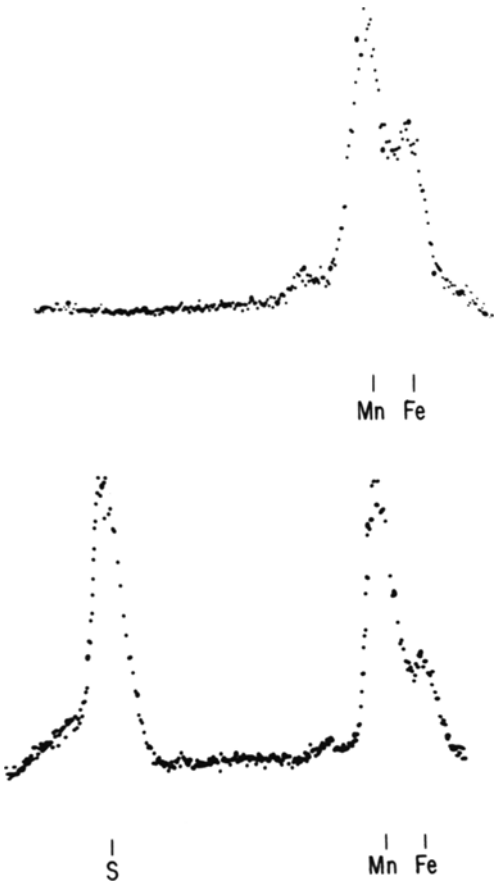

Fig. 15—Fluorescent X-ray spectra of Mn(Fe)O (top) and Mn(Fe)S (bottom) inclusions on the fracture surface of Fe-1.1 pct Mn-0.14 pct S-0.04 pct O alloy.

or no change in the manganese concentration of the metal.

In the foregoing analysis, it is assumed that the liquid oxysulfide is saturated with "MnO" throughout the progress of solidification. Of course, this may not necessarily be the case. Depending on the manganese content and the ratio %O/%S in the melt, the first inclusion formed during freezing could be the oxide, sulfide, or the liquid oxysulfide. From the "MnO" and "MnS" solubility products, it is predicted that at high manganese contents (greater than about 1 pct Mn for which a_{MnS} and a_{MnO} are close to unity) and at the freezing temperature of 1525°C, "MnO" forms first when (%O/%S) > 0.087 which is the case in the example considered above.

Polished sections of the quaternary alloy investigated look much like that for the Fe-0.14 pct S-0.04 pct O ternary alloy shown in Fig. 9. The fracture surfaces of the quaternary alloys are shown in Fig. 14 at low and high magnifications. Typical examples of the fluorescent X-ray spectra obtained from several inclusions in different regions on the fracture surface are given in Fig. 15 showing that some inclusions are Mn(Fe)O and some Mn(Fe)S. The amount of iron associated with the oxides and sulfides cannot be estimated from the fluorescent X-ray spectra because of the X-ray scattering from the metal surrounding the inclusion. Of the five inclusions in Fig. 14 (bottom), one at the center and one at the extreme left are "MnS" and the other inclusions are "MnO". These observations substantiate the view once again that the oxides and sulfides formed in the enriched liquid during freezing are trapped within growing dendrite branches and are not pushed into the main interdendritic region. When the oxygen and sulfur concentrations are low, *e.g.* ~0.01 to 0.015 pct as in most steels, the oxysulfide inclusions form only at the later stages of freezing, *e.g.* beyond about 95 pct solidification; hence on the polished and suitably etched sections of the casting, small inclusions may act as markers delineating the position of the interdendritic regions, Figs. 12 and 13.

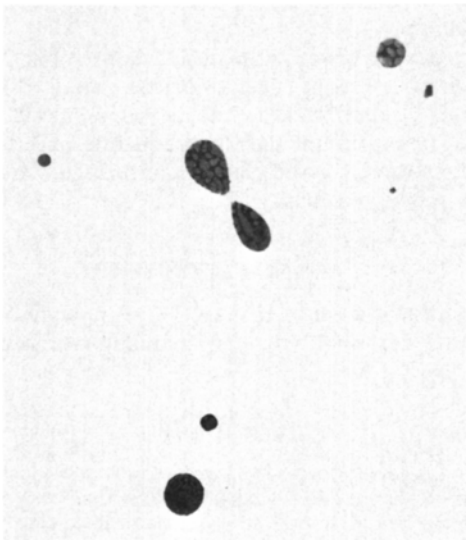

Fig. 16—Micrographs showing "MnS"-"MnO" eutectic freezing of liquid oxysulfide in Fe-1.1 pct Mn-0.17 pct S-0.03 pct O alloy, annealed for 1 hr at 1450°C and water quenched. Inclusion growth during the anneal is indicated by the presence of inclusion depleted zone around large oxysulfide spheroids.

Samples of the manganese alloy investigated, contained in evacuated silica capsules, were annealed for 1 hr at 1450°C and water quenched. This treatment resulted in appreciable growth of the inclusions which, as seen from the micrographs in Fig. 16, appear to have been molten at the annealing temperature, in accord with the equilibrium diagram in Fig. 3. The manganese-sulfide inclusions (grey) were obviously formed at the eutectic univariant *h* during the water quench. The growth of inclusions during the high-temperature anneal is also evidenced from the depletion of small inclusions around the large oxysulfide spheroids, faintly detectable in Fig. 16.

CONCLUSIONS

The phase relations in Mn(Fe)O-saturated Fe-Mn-S-O calculated from available data and some theoretical considerations are verified by differential thermal analysis of three alloys containing 1.1, 3.3, and 4.8 pct Mn, together with some sulfur and oxygen. It is found that the α-γ, γ-δ and solidus temperatures are similar to those of the Fe-Mn manganese binary system. The univariant for the γ-iron/"MnO"/"MnS"/liquid oxysulfide equilibrium, estimated from thermodynamic principles, is verified experimentally. This univariant extends from the eutectic invariant at 900°C with 10

ppm Mn in solution in the metal to about 1220°C at about 90 pct Mn.

Microscopic observations on fracture surfaces (using electron microscopy) and etched sections of Fe-S-O, Fe-Mn-S-C, and Fe-Mn-S-O alloys substantiated the mode of formation of the oxide, sulfide and oxysulfide inclusions during solidification anticipated from a simple conceptual analysis.

ACKNOWLEDGMENT

The authors wish to thank C. E. Brickner of this laboratory for work with the scanning electron microscope.

REFERENCES

1. E. T. Turkdogan and G. J. W. Kor: *Met. Trans.*, 1971, vol. 2, pp. 1561-70.
2. W. Hume-Rothery and R. A. Buckley: *J. Iron Steel Inst.*, 1964, vol. 202, p. 534; A. Hellawell and W. Hume-Rothery: *Phil. Trans. Roy. Soc. London*, 1957, vol. 249, pp. 417-59.
3. J. F. Elliott, M. Gleiser, and V. Ramakrishna: *Thermochemistry for Steelmaking*, Addison-Wesley Publ. Co., Inc., Massachusetts, 1963.
4. F. Körber: *Stahl Eisen*, 1936, vol. 56, pp. 433-43.
5. H. Wentrup: *Tech. Mitt. Krupp*, 1937, vol. 5, pp. 131-73.
6. R. Vogel and W. Hotop: *Arch. Eisenhüttenw.*, 1937, vol. 11, pp. 41-54; Brutcher Trans. No. 459.
7. G. W. Morey and E. D. Williamson: *J. Amer. Chem. Soc.*, 1918, vol. 40, pp. 59-84.
8. L. S. Darken: *J. Amer. Chem. Soc.*, 1948, vol. 70, pp. 2046-53.
9. T. Rosenqvist and B. L. Dunicz: *Trans. AIME*, 1952, vol. 194, pp. 604-08.
10. E. T. Turkdogan, S. Ignatowicz, and J. Pearson: *J. Iron Steel Inst.*, 1955, vol. 180, pp. 349-54.
11. S. Speil, L. H. Berkelhamer, J. A. Paak, and B. Davis: *U. S. Bur. Mines*, Tech. Paper 664, 1945.
12. P. F. Kerr and J. L. Kulp: *Amer. Mineral.*, 1948, vol. 33, pp. 387-419.
13. A. R. Troiano and F. T. McGuire: *Trans. ASM*, 1943, vol. 31, pp. 340-59.
14. D. C. Hilty and W. Crafts: *Trans. AIME*, 1954, vol. 200, pp. 959-67.
15. E. T. Turkdogan: *Trans. TMS-AIME*, 1965, vol. 233, pp. 2100-12;
16. J. Yarwood, J. F. Elliott, and M. C. Flemings: *Met. Trans.*, 1971, vol. 2, pp. 2573-82.
17. D. C. Hilty and W. Crafts: *Trans. AIME*, 1952, vol. 194, pp. 1307-12.
18. E. T. Turkdogan and R. A. Grange: *J. Iron Steel Inst.*, 1970, vol. 208, pp. 482-94.
19. E. Scheil: *Z. Metallk.*, 1942, vol. 34, pp. 70-72.